Available Online at http://www.journalajst.com

ASIAN JOURNAL OF SCIENCE AND TECHNOLOGY

ISSN: 0976-3376

Asian Journal of Science and Technology
Vol. 16, Issue, 08, pp. 13852-13861, August, 2025

RESEARCH ARTICLE

QUANTIFYING FAULT REACTIVATION RISK IN THE DEEP OFFSHORE NIGER DELTA USING GEOMECHANICAL MODELLING

Mary Abiodun Ajibade*[1] and Mary Taiwo Olowokere[2]

[1]Department of Applied Geophysics, Olusegun Agagu of Science and Technology, Okitipupa, Nigeria
[2]Department of Applied Geophysics, Federal University of Technology, Akure, Nigeria

ARTICLE INFO

Article History:
Received 18th May, 2025
Received in revised form
27th June, 2025
Accepted 28th July, 2025
Published online 30th August, 2025

Keywords:

Geomechanical,In-situ stress, structural modelling, fault model,fault reactivation, Fracture Stability, Slip tendency, Dilation tendency, geomechanical attributes, Pore Pressure, stress distribution.

Corresponding author: Lie Chun Pong,

ABSTRACT

A number of large petroleum fields are located in anticlinal structures within the Niger Delta, and these fields may be considered as potential fault reactivation risk as time goes on. High resolution predictive model was generated in this study using 3D finite element models constrained by seismic with a view to improving wellbore stability predictions along the paths of future development wells. 3D seismic data, borehole and production data were integrated in the analysis and interpretation of detailed structural model of the study area. The study performed geomechanical modelling to assess the likelihood of fault reactivation since both normal faulting regimes exist in the study area. Reservoir geomechanical data indicates that the in-situ stress in this region is characterised by normal faulting conditions where S_V (75 MPa/km) >S_{Hmax} (68.5 MPa/km) >S_{hmin} (40 MPa/km). The results show northwest to southeast and east-northeast to west-southwest fault trending that are presently at moderate and high risks of reactivation. The results also reveal thatfault reactivation potentialcan beinfluenced faultbysurface geometryand thus development of detailed reservoir structural models is importantfor risk assessments before future wells development.

Citation: ***Mary Abiodun Ajibade and Mary Taiwo Olowokere.*** **2025.** "Quantifying Fault Reactivation risk in the deep Offshore niger Delta Using Geomechanical Modelling", *Asian Journal of Science and Technology*, 16, (08), 13852-13861.

INTRODUCTION

In this study, geomechanical modelling is used to analyse the fault reactivation and fracture opening risk along faults from the northwestern part 'Kings' Field, Offshore Niger Delta. The north-northwest to south-southeast and east-northeast to west-southwest oriented faults have the highest risk to slip, whereas northeast to southwest oriented faults experience low likelihood of reactivation under the existing stress regime. The study presented a low risk of fault reactivation in the Central part based on the regional stress regime and also demonstrated that the highest risk of faults reactivation is under a normal faulting scenario. The study showed the importance of the detailed fault modelling, which highlights fault plane variations along strike and how it affects the risk of faultreactivation. This fault model can also be applied as a proxy in the deep offshore part of the Niger Delta, where the geological information needed for fault reactivation analysis is limited.

Field Location: This study was carried out using deepwaterBonga Field, located 120 kilometres offshore in the Gulf of Guinea (Figure 1), is the first major deepwater field operated by Shell in West Africa in partnership with ExxonMobil, Total and Agip, and under Production Sharing Contract with NAPIMS. Water depths at Bonga ranges from 945-1158 meters (3100-3800 ft).

Background and Overview

Previous Works: The Reservoir Characterization Project has a long and storied history of using geomechanics as a high-tech reservoir characterization tool for both conventional and unconventional studies. Within the last decade, several theses have come out of this group focused on the geomechanical characterization of tight oil and gas plays. This study has been built around a strong interdisciplinary dataset. The reason geomechanical studies are carried out in the field of petroleum geophysics can be attributed to the strong effect that in-situ rock strengths and stresses have on production. Different scales of heterogeneity and anisotropy are sources of change for reservoir properties and production across a field and even within a small study area such as the one 'Bon' is currently evaluating. 'Bon' Field, in particular, is riddled with normal faults forming en-echelon graben systems at the reservoir level throughout the entire field which will affect in-situ stress. Apart from the subsequently cited publications, the field of reservoir geomechanics is comprehensively described and summarized by Zoback (2007). Fjaer et al. (2008) provides a more general overview on petroleum-related rock mechanics. Since the mid 1990's, the importance of tectonic in situ stresses in subsurface operations has been increasingly recognized in science and industry – especially the impact on optimal exploitation of hydrocarbon reservoirs. This is mostly due to expensive operational failure and the demand for more efficient exploitation of conventional reservoirs.

A study published by Yale (2003) showed several examples for the stress distribution in reservoirs. He analyzed local perturbations of the regional stress field focusing on the influence of faults and horizontal stress magnitudes. Intense faulting and strong segmentation of reservoirs can result in stress decoupling in individual fault blocks and stress deviations of up to 90° from the regional trend (Yale, 2003).

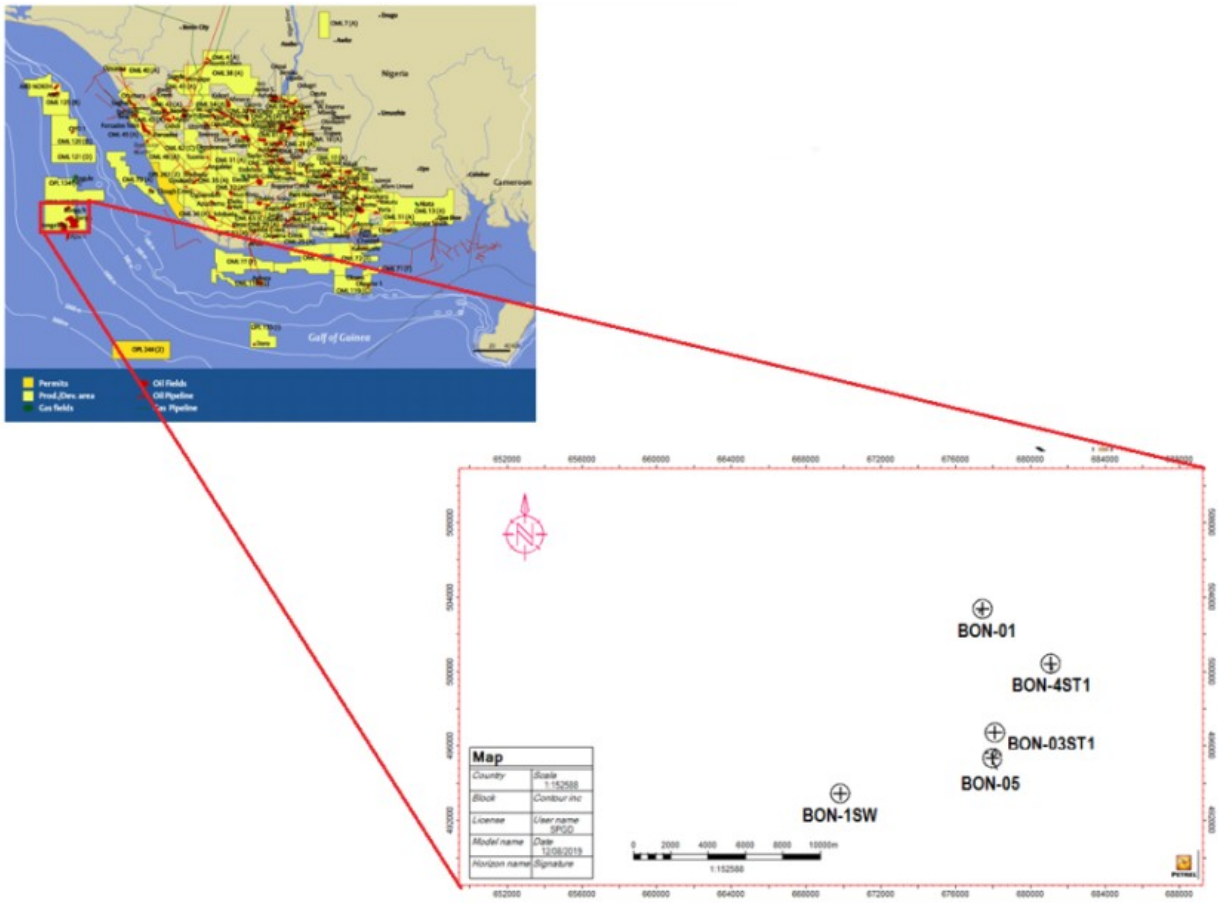

Fig. 1. Diagram showing the location of studied area and the Niger Delta mega-structural framework (modified from Ejedavwe et al. 2002)

First geomechanical models using the Finite Element Method (FEM) and incorporating simple reservoir geometries are published by Bourne et al. (2000), Fredrich et al. (2000, 2003), and van Wees et al. (2003), for instance. Bourne et al. (2000) used a combined approach of geomechanics and flow simulation to model naturally fractured reservoirs in 3D. By constraining and validating the model with seismic data, well tests and production data, uncertainties were significantly reduced and it was possible to pre-estimate physically and geologically realistic fracture networks. One of the first geomechanical models, which incorporated a more sophisticated 3D reservoir structure including faults, was the work of van Wees et al. (2003). The simulation of gas depletion predicted a stabilization of the stress field and a reduced likelihood of failure for reservoirs in compressive and strike-slip regimes. The application to a case study reservoir in Northern Germany illustrates the general potential of this geomechanicalmodelling approach. The derivation of area-wide rock mechanical parameters from seismic data represents a promising next step for significant improvement of geomechanical models – especially those using the finite elements. Although the principles for deriving such parameters are outlined (e.g. by Gray et al. (2012)), the respective data is yet commonly scarce. Herwanger and Koutsabeloulis (2011) provided a guideline to build and calibrate geomechanical FE models with such 3D and even 4D seismic data. Highly sophisticated FE models on field-scale can be built using this same data. Longuemare et al. (2002) modelled the influence of production-induced geomechanical effects on fluid flow at a case study by using a partially coupled approach. The results indicate progressive strain localization on a limited number of faults when the mechanical equilibrium of the reservoir is disturbed during production. Stearns and Friedman reviewed the multiple roles played by fractures in exploration and exploitation of naturally fractured reservoirs (Stearnsand Friedman, 1972). They showed that fractures could alter the matrix porosity or the permeability, or both. Sathyamoorthy *et al*. (2009), presents key elements of successful WRM in Bonga. The study showed the factors to include people factor and cross discipline integration, Smart Fields® capability, 'live' WRM Plan and monitoring, good understanding of subsurface, application of integrated production modelling, intervention readiness and effective well integrity management. The paper concludes on key learning applicable to future deepwaterwater flood projects. This current study differs from the existing literature in its strong focus on creating a 3D geomechanical model to understand stress changes and heterogeneity throughout reservoir.

Overview of study area

Regional Geology: The Tertiary Niger Delta Basin located in southern Nigeria at the inland margin of the Gulf of Guinea is situated at the southernmost extremity of the elongated intra-continental Benue Trough. It is situated between latitudes 3° and 6°N and longitudes 5° and 8°E (Fig. 2). The basin is bounded by the Calabar Flank in theeast, Benin Flank in the west, Gulf of Guinea in the south and in the north by older (Cretaceous) tectonic elements such as the Anambra Basin and Afikpo Syncline (Avbovbo, 1978; Ejedawe et al., 1984; Tuttle et al., 1999). The evolution of the Niger Delta basin is controlled by pre- and syn- sedimentary tectonic activities described by Evamy et al., (1978), Ejedawe et al., (1984), and Knox and Omatsola, (1989).

The pre-sedimentary tectonic activities generated Cretaceous Fracture zones commonly expressed as trenches and ridges in the deep Atlantic. The fracture zones subdivide the West African Shield into individual basins, and in Nigeria, the fault zones form boundary faults that generated the Cretaceous Benue—Abakaliki Trough which is a failed arm of a rift triple junction associated with the opening of the south Atlantic (Lehner and De Ruiter, 1977). Syn-sedimentary tectonic activities shaped the internal geometry of the basin and include gravity tectonics which became active after the rifting episode. The gravity tectonic event is expressed in complex sedimentary structures in the form synthetic and antithetic growth fault, roll-over anticlines and salt diapirs among others (Fig. 3).

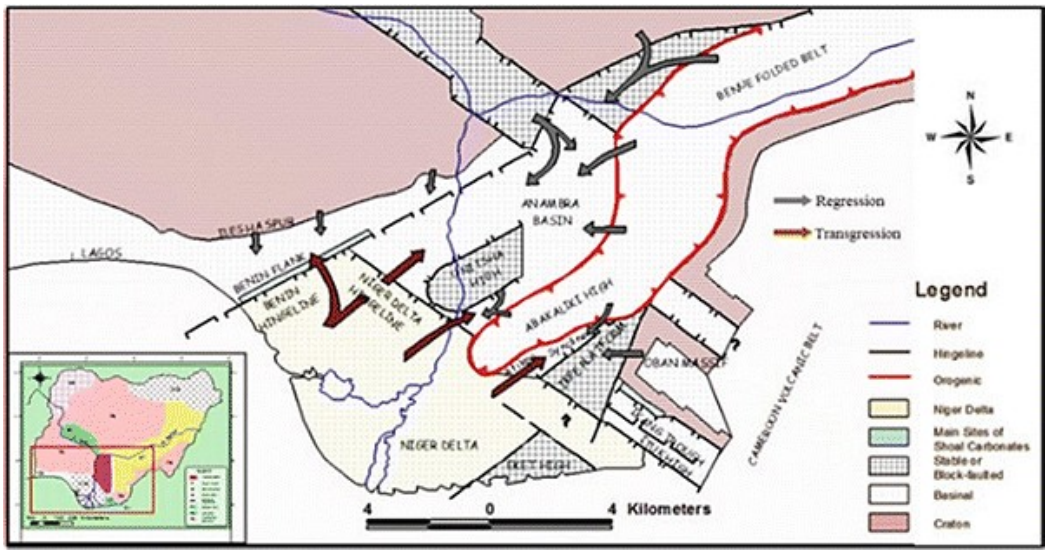

Fig. 2. Tectonic setting and structural elements of the Niger Delta Basin (Kogbe, 1989)

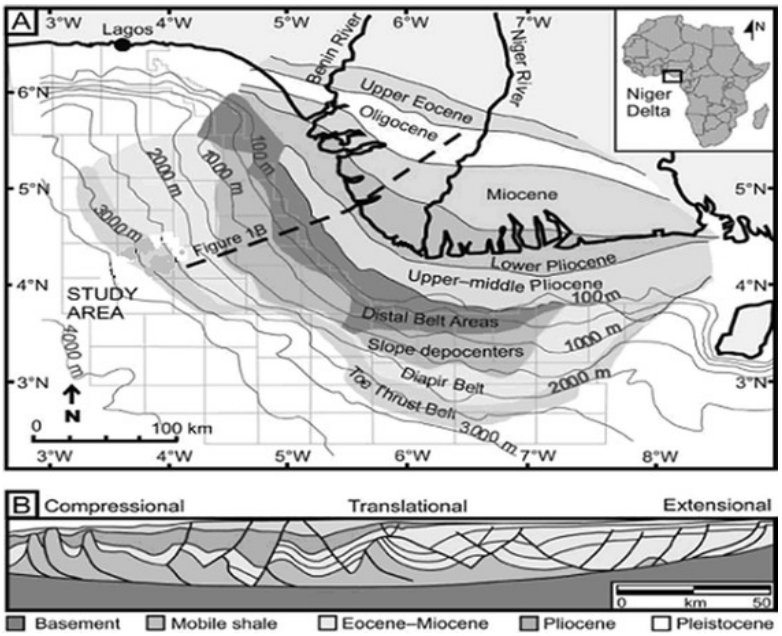

Fig. 3. The Niger Delta complex showing the continental shelf, slope and rise showing Structural domains of Niger Delta (Cohen and McClay, 1996)

Regional Stratigraphy: The sedimentary fill of the Niger Delta Basin is divided into three diachronous formations, namely the Akata Formation, Agbada Formation and Benin Formation (Fig. 3). The Akata Formation is typically under compacted, overpressured and made up of prodeltashales with occasional turbidite sands. It also provides the detachment horizon for large growth faults that define depobelts (Adeogba et al. 2005). The Agbada Formation consists of paralic, mainly shelf deposits of alternating sands, shales and mudstone. The Benin Formation is predominantly non-marine upper delta plain sandstone. The total sedimentary sequence was deposited in a series of mega-sedimentary belts (depobelts or mega-structures) in a succession temporally and spatially with southward progradation of the Delta (Doust and Omatsola, 1990). Reservoir intervals in the Agbada Formation have been interpreted to be deposits of highstand and transgressive systems tracts in proximal shallow ramp settings (Evamy et al., 1978). Structural traps formed during syn-sedimentary deformation of the Agbada Formation (Evamy et al., 1978), and stratigraphic traps formed preferentially along the delta flanks, define the most common reservoir locations within the Niger Delta complex (Rowlands, 1978). The primary seal rocks are interbeddedshales within the Agbada Formation. Three types of seals are recognized: clay smears along faults, interbedded sealing units juxtaposed against reservoir sands due to faulting, and vertical seals produced by laterally continuous shale-rich strata (Doust and Omatsola, 1990). The Niger Delta basin has area coverage of about 75,000 km^2 and consists of an overall regressive clastic sequence which reaches a maximum thickness of about 12,000 m in the central part of the basin where there is maximum subsidence (Merki 1972). The basin consists of progradational, paralic sequences of Akata, Agbada and Benin Formations which builds southwards into the deep waters and this account for the Delta Complex in the Oligocene–Miocene times (Doust and Omatsola 1990).

Regional Structural Geology: The structural framework of the basin as controlled by basin geometry, rate of sedimentation and the progradation of sandy deposits over under-compacted delta marine shale is dominated by many syn-depositional structural signatures associated with gravity tectonics. Structural and stratigraphic traps are the main traps in Niger Delta (Figure 5). Growth faults, rollover anticlines and diapiric structures are the prevailing structural styles in the Niger Delta Basin. Growth faults are the dominant structural features in the Niger Delta (Opara et al., 2008; Magbagbeola and Willis, 2007). Most hydrocarbon-bearing structures are along proximal margins of sub basins where growth strata accumulated on blocks downdropped across major syndepositional faults and onlap

adjacent anticlinal (rollover) closures (Doust and Omatsola, 1990). Source rocks in the Niger Delta might include marine interbedded shale in the Agbada Formation, marine Akata Formation shales and underlying Cretaceous shales (Evamy et al., 1978; Ekweozor and Okoye, 1980; Doust and Omatsola, 1990).

depth-migrated 3D reflection seismic data set. The average dominant frequency of data was 30 Hz. The seismic data were used to detect subtle faults and large-scale fractures. Geophysical logs of AC, DEN, CN, and GR from 6 wells (BON--01, BON-3ST-1, BON-04, BON-4ST1 and BON-05) were collected and used in this study.

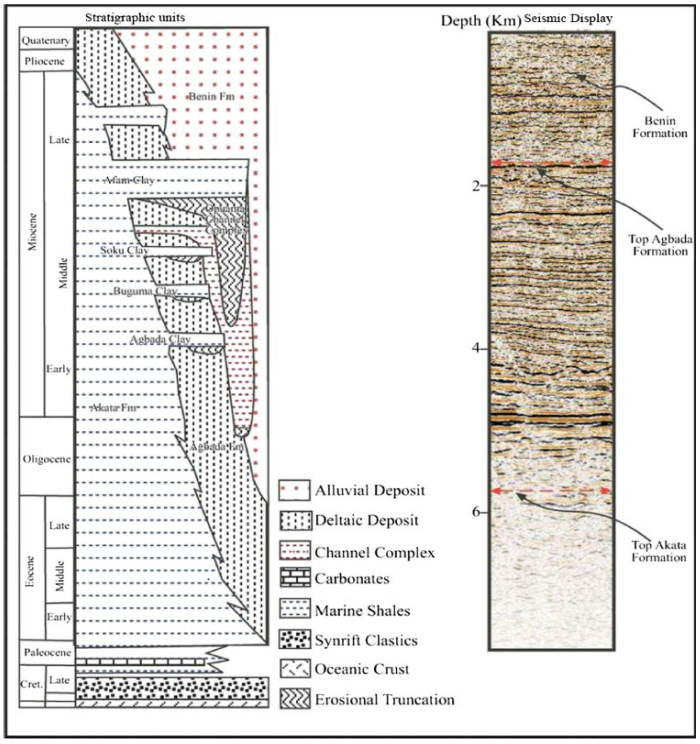

Fig. 4. Stratigraphy of the Niger Delta and variable density seismic display of the main stratigraphic units (Lawrence et al 2002)

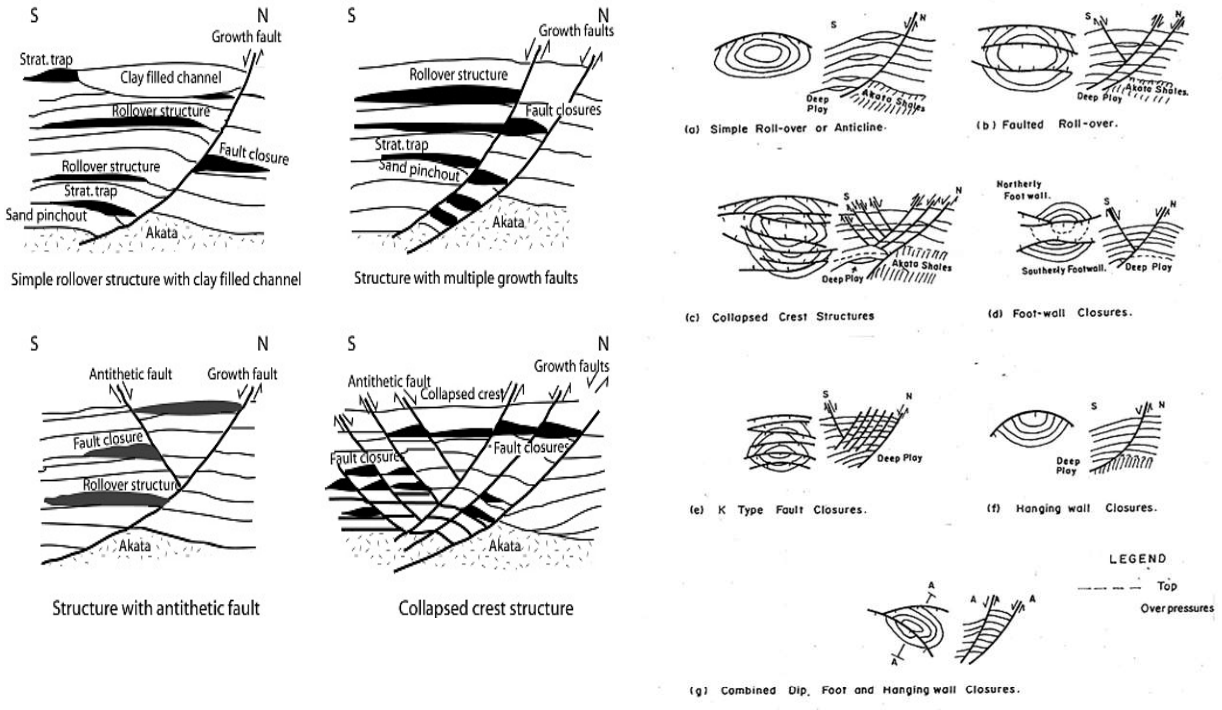

Fig. 5. Examples of Niger Delta oil field structures and associated trap types (Modified from Doust and Omotsola, 1990 and SPDC, 1991).

METHODS AND MATERIALS

The 3D seismic dataset was used to create a structural model of the study area (Fig. 1). The study field is covered by 3D seismic data with an area of ~1814 km^2 that was acquired in 2008, and reprocessed though pre-stack depth migration in 2012. We analysed the pre-stack,

The 6 m cores from two cored wells (locations are shown in Figure 1) were observed and analysed. Geophysical logs and core observation data were used to identify the features, e.g., fracture density and fracture dip angle of small-scale fractures at the borehole scale

Structural Model: Structural interpretation was conducted every 10–20 inlines with the help of crosslines and arbitrary lines, depending on

the complexity of the fault plane geometry. Lateral resolution of fault planes can be estimated based on a bin size between 250–500 m, which seems to be a good approximation between the study area size and resolution of geomechanical modelling. Interpretation of 3D fault surfaces had not been undertaken across the entire study field. According to (Morley etal al., 2006) 3D fault surfaces interpretation improves understanding of the way different fault surfaces evolve through time. In this study, maximum positive curvature, apparent dip, and similarity attributes were calculated and incorporated into the structural interpretation. Of these attributes, similarity and dip were utilized to give detail of the lateral continuity of the fault planes at different depths.Structural and facies models of the study area within the reservoir of interest are shown in Figure. 6a and b.The mesh grill top and bottom (blue and yellow) is model boundaries, the different coloured vertical pillars are the faults interpreted along the entire 3D structural grid. Horizons are color-coded by depth. Faults are individually assigned a unique colour automatically. Following initial interpretation, all fault planes were meshed, creating an irregular grid and keeping the original location of fault sticks in the same position.

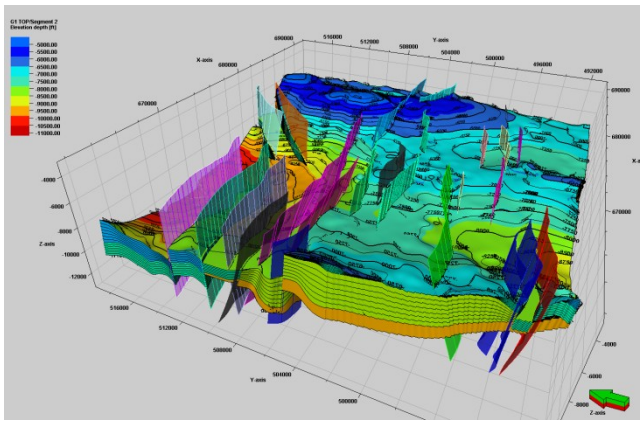

Fig. 6a: 3D view of the structural framework of the model

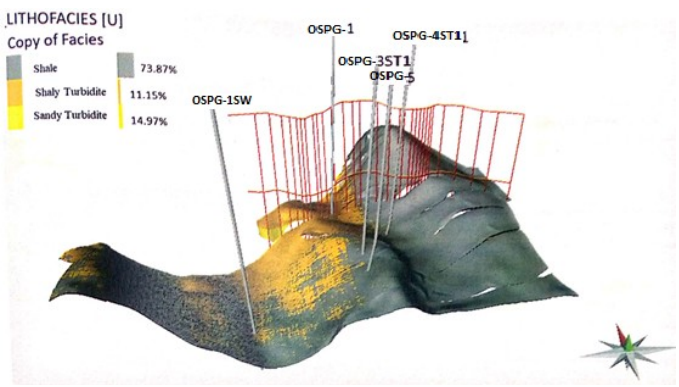

Fig. 6b. 3D view of the facies model

Determination of the in-situ stress: In-situ stress can be expressed by the vertical stress(S_v), maximum horizontal principal stress(S_{Hmax}), and minimum horizontal principal stress (S_{hmin}) under the ground. Similary, there is a relationship between the effective stresses and the pore pressure. Vertical stress was calculated using bulk density logs and the horizontal stress were measureddirect from LOTs (leak-off tests), XLOTs (extended leak-off tests).

Vertical stress (S_v): Gravitational loading at any point in the earth is caused by the weight of the rock column overlaying that point. The overburden stress (S_v) at depth, z, is calculated by integrating the weight above the point (z) using the following equation:

$$S_{v=\int_0^z(\rho(z)*g)dz} \quad \text{.....(1)}$$

Where,

S_v: vertical / overburden stress, ρ(z): formation bulk density, g: gravitational acceleration
z: depth (true vertical depth)

In the study area, the magnitude of the total overburden gradient was obtained by integrating the available density logs with depth along the well paths of the ten keywells shown in Table 1. Since the formation bulk density log is not available to the surface, an exponential curve was used to fit the measured data and to calculate the formation density using the Gardner formula. In some sections, where the density data is unreasonably low or high (due to poor quality density log from an enlarged hole), the density log is interpolated by a best-fitline or by using pseudo density from the acoustic log using the Gardner's relationship .

Minimum Horizontal stress Magnitude: The magnitude of the total minimum horizontal stress (S_{hmin}) was estimated using the mud weight (MW), and formation integrity pressure (FIP) are often recorded in daily drilling or well completion reports, and can also be useful to constrain S_{hmin}. In this context, a lower bound value for the magnitude of the minimum horizontal stress (S_{hmin}) can be approximately evaluated using the FIP, as in Equation 2.

$$S_{hmin} = (MW\ X\ 9.81\ X\ Z) + (FIP) \quad (2)$$

In Equation 2, S_{hmin} is the magnitude of the minimum horizontal stress, MW is the mud weight, Z is the depth of the FIP is the formation integrity pressure. We used formation integrity pressure (FIP) because there is no leak-off tests (LOTs) data. The purpose of conducting a FIT is to test the formation fracture pressure required for kick tolerance and/or safe drilling mud weight margin. The maximum pressure in the FIT test is less than the fracture initiation and formation breakdown pressures.

Maximum horizontal stress magnitude: The maximum horizontal stress (S_{Hmax}) magnitude was evaluated by an integrated analysis of the occurrence of borehole breakouts (BOs), drilling-induced tensile fractures (DITFs), and the knowledge of compressive or tensile rock strength. In the absence of rock strength data, the upper limit of the S_{Hmax} magnitude can be estimated by the frictional limits theory, which establishes a relationship between the maximum and the minimum stress (Eq. 3). Because there is no rock strength data available for wells in this study area, the frictional limits theory is used to estimate the upper limit of the S_{Hmax} magnitude.

$$\frac{S_{HMAX} - P_p}{S_{hmin} - P_p} \leq \left\{\sqrt{\mu^2 + 1} + \mu\right\}^2 \quad \text{..... (3)}$$

In Equation 3, μ is the coefficient of friction on an optimally oriented fault surface, most commonly of a value of 0.6~0.8 (Byerlee, 2016). Using a conservative value of 0.6, the maximum horizontal stress gradient in the study area is about 40.65 MPa/km. (0.65, 0.78)

$$S_{Hmax = S_{hmin}(Z_d)} = \frac{\mu}{1-\mu} S_v(Z_d) \quad \text{.....(4)}$$

Where S_V (Pa), S_{Hmax} (Pa), and S_{hmin} (Pa) are the vertical, maximum horizontal, and minimum horizontal principal stresses (respectively); zd (m) is the depth; g(m·s^{-2}) is the vertical component of the gravity acceleration; ρ(kg·m^{-3}) is the rock mass density, and μ is Poisson's ratio.

This paper used seismically-derived 3D structural framework to establish the geomechanical risk associated for the RFS following a potential increase in pressure associated with the injection of CO_2. The geomechanical attributes (fracture stability, slip tendency, and dilation tendency) for the faults were calculated. The calculated geomechanical attributes are displayed on the interpreted fault planes, providing a direct visualisation of the areas at a higher risk of brittle failure.

Pore Pressure Estimation: To complete the determination of stress state (Figure 7), knowledge about pore pressure is required. Direct measurements of formation pressure were obtained by direct measurement from repeat formation tests/RFTs.

Slip tendency analysis: Reactivation of pre-existing faults may create leakage conduits that will risk the seal capacity in an injection project. The slip will occur on a fault when the maximum shear stress acting on the fault plane exceeds the shear strength of the fault. Slip tendency is a method that allows quick assessment of stress states and related potential fault activity (Morris et al. 1996). The assumption that slips is likely to occur on a planar surface when the resolved shear stress acting on this surface is equal or higher than the frictional resistance to sliding was defined by (Morris et al, 1996); by Eq. 5).

$$T_s = \frac{\tau}{\sigma_n} \qquad (5)$$

Whereτ is shear stress, σ_n is the normal effective stress acting on the dislocation surface, and τ_s is the likelihood that a fault or fracture will undergo slip.

The results of the slip tendency analysis are displayed on the 3D structural model. The slip tendency results are colour coded from 0–1, where the higher the value is, the greater likelihood of fault slip by shear fracturing is.

Dilation tendency analysis: The aim of applying the dilation tendency attribute to this structural model was to determine the sections of the reservoir segments that are more prone to allowing fluid migration in the fault plane. The normal stress on a fault or a fracture depends on the magnitude and direction of the principal stresses relative to the fracture plane. The ability of a fault or fracture to dilate and transmit fluid is directly related to its aperture, which is a function of the effective stress acting upon it is defined by Ferrill etal. (2020) by the following Eq. (6):

$$T_d = \frac{\sigma_1 - \sigma_n}{\sigma_1 - \sigma_3} \qquad (6)$$

whereσn is the resolved normal stress, $\sigma 1$ is the maximumprincipal compressive stress, and $\sigma 3$ is the minimum principal compressive stress.

RESULTS AND DISCUSSION

In Situ Stresses Profile: The calculated magnitudes of the three principle stresses in the Bonga Field resulted that, Shmax was found to be the higher principle stress, and the magnitude of the vertical stress was found to be greater than the minimum horizontal stress, indicating that a normal stress regime (Sv>Shmax>Shmin) dominates the field (Fig. 7).

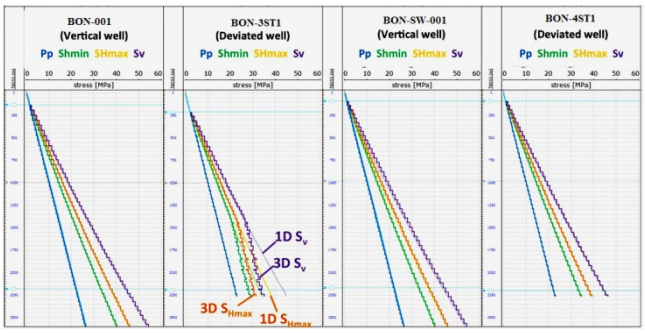

Fig. 7. Pressure Profile and Stress profiles in BONwells indicating a normal stress regime (Sv>Shmax>Shmin). The blue circles represent the formation fluid pressures (RFT), and triangles indicate FIT pressure (the stresses are calculated using the elastic moduli estimated by the empirical equations.

This result is consistent with the earlier findings of (Adewole and Healy, 2013). The calibrated stress profiles for the BON-3ST1 well (shown in Fig. 7) was prepared for interpolation into the geomechanical model, and the stress initialization distribution in the geomechanical model is shown in Figure 8. Figure 8 show the 3D Stress distribution inside the reservoir layer in the vicinity of the wells in the study area. Figure 8: 3D Stress distribution inside the reservoir layer in the vicinity of the wells in the study area. The colour scale show the maximum strain in red and minimum strain in Purple blue. The boundary conditions for the global model were set as fully constrained bottom and lateral surfaces.

In situ stress magnitude: Figure 9 shows the 3-D view of PP, Sv, Shmax and Shmin models of Miocene to Pliocene Agbada Formation reservoirs using Well BON-3ST1 . Each geobody represents the spatial distribution of each property within the formation along the X-Y-Z axis of the modelled grid.The distribution trend of S_{hmin} magnitude was similar to that of S_{Hmax}, that is, lower in the central part and fault zone and higher in the surrounding area. The magnitudes were mainly between 30–80 MPaand the average stress gradient was 1.47 MPa/100 m. For vertical principal stress, the magnitudes were about 70–90 MPa, and the average stress gradient was 2.25 MPa/100 m. Overall, horizontal differential stress did not exceed 30 MPa and was generally below 20 MPa. From the calculated horizontal stress from the LOT and XLOT data, the maximum horizontal principal stress is less than or equal to the vertical stress, indicating a stress regime between a normal faulting (Sv>SHmax>Shmin) and transition stress regime (Sv ≈ SHmax>Shmin) in the study field.

In situ stress orientations: The general trend of S_{Hmax} in the study area was NEE–SWW to SEE–NWW with a measured range between 58°–238° and 103°–283°. In the central region of the study area, the S_{Hmax} show a close to E–W trend, the value ranges from 75°–255° and 96°–276°., the distribution trend of S_{Hmax} in the western part of the studyis NE–SW, with the value of S_{Hmax}ranging between 58°–238° and 88°–268°. The distribution trend of S_{hmin} and S_{Hmax} were perpendicular with the general trend of S_{hmin} from NNW–SSE to NNE–SSW. Thetrend of S_{Hmax} was relatively uniform withconstant variationswithin the same fault block, but there are changes in trend observed between different fault blocks. The non-uniform stress orientations were as a result ofheterogeneity of lithofacies and fault distribution. Lithofacies heterogeneity results in small but consistent stress orientation changes within a fault block; fault distributionresults in large deflections of the stress orientation. Therefore, there were large differences in stress trend between fault blocks.Figure 10 shows the distribution of PP, Sv, Shmax and Shminon fault faces. The measured and modelled magnitudes of both horizontal stresses were compared and show that the respective deviations are always less than 4MPa. It also indicates the improvement due to calibration by additionally plotting the results of the default model (Fig. 11).

The Faults and fracture Movement Behaviour : Estimates of the stress sensitivity of each fracture were determined using the ratio of calculated shear stress, τ, and the critical shear stress, τ_{max} which is referred to as Slip tendency (τ_{ratio}). τ_{ratio} lies between 0 and 1. It identifies the fracture sets that are optimally oriented to slip and are therefore the most likely to have enhanced permeability. The dilation tendency provides a ranking criterion highlighting which fracture orientations are more likely to be open and therefore able to transmit fluids. Figure 12 shows Mohr circle diagram demonstrating the calculations involved with the three different stress attributes modelled.

Reactivation Tendency of Faults and Fracture stability analysis: The stress field defined for average reservoir depth i.e. 2500m was displayed as semi-Mohr circles with fracture envelope for fault rock for the average reservoir depth. The coefficient of friction (μ) was taken as 0.6 and the cohesiveness value. The poles of the E-W and NE-SW faults were plotted on Mohr's diagram.

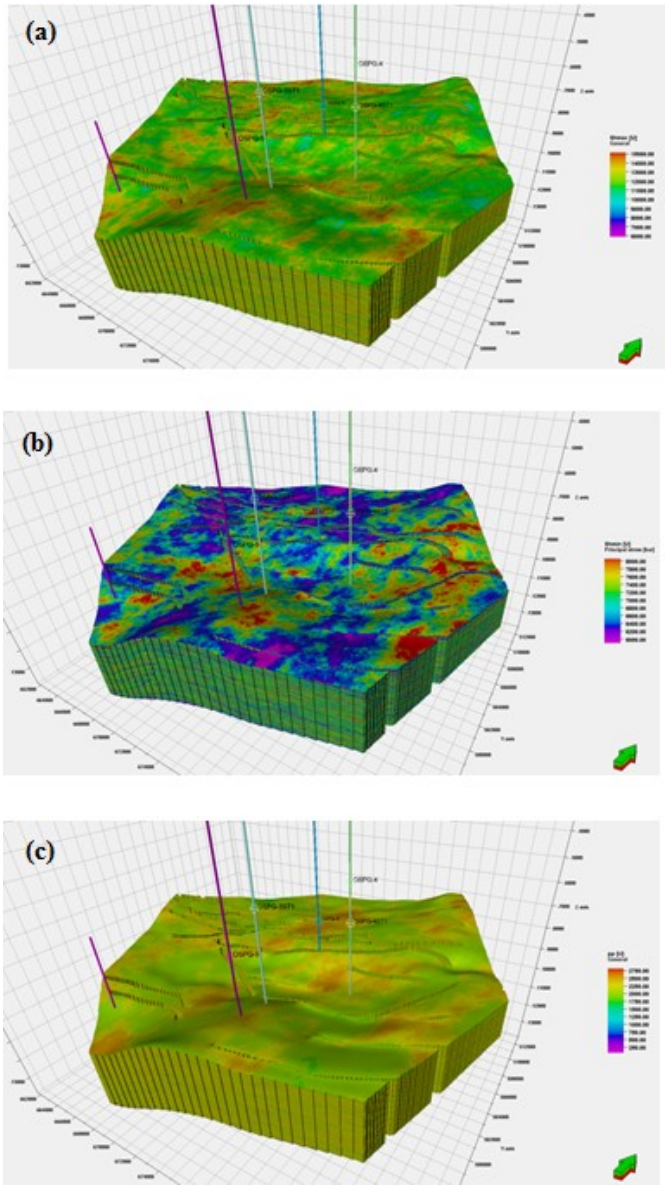

Figure 8: 3D Stress distribution inside the reservoir layer in the vicinity of the wells in the study area. (maximum strain is red and minimum strain is Purple blue).

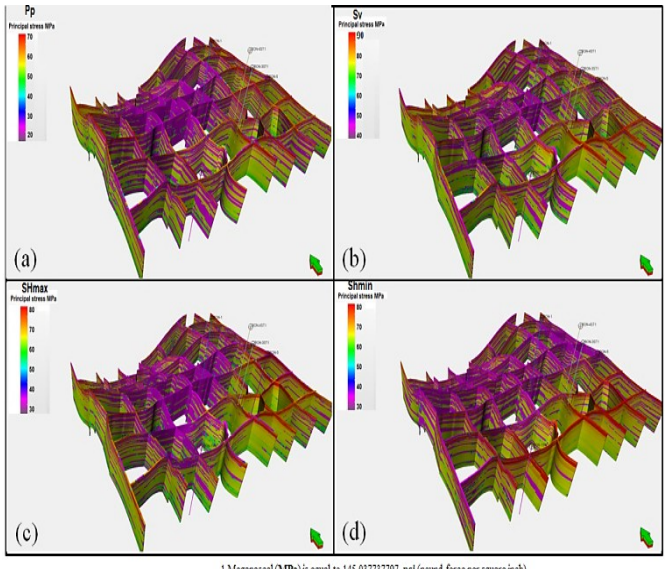

Fig. 9. 3-D view of PP, Sv, Shmax and Shmin models of Miocene to Pliocene Agbada Formation reservoirs

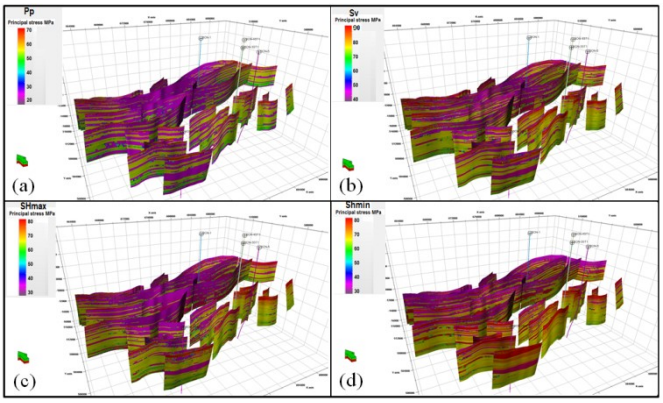

Figure 10. Spatial distribution of PP, Sv, Shmax and Shminon fault faces [MPa]

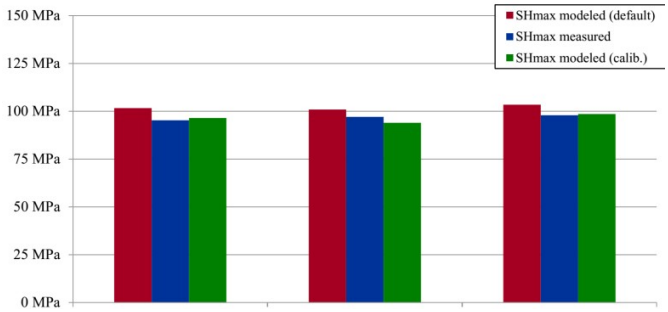

Fig. 11. Diagram comparing the measured magnitudes of the maximum horizontal stress (SHmax) with the values of the default and calibrated geomechanical model

Stereo plotsthat displayzones of high or low values for slip tendency, slip Stability, fracture stability and dilation tendency were generated. The poles of fault were plotted on the stereograms of all the geomechanical attributes for seal integrity. Figure 13 to 15 show the Mohr diagram and stereogram of Δp using the Coulomb failure envelope of μ = 0.6 at reservoir depths of 2500 m and 3000m. Red arcs on the stereogram represent two optimal fault orientations (−17.5°∠60° and 162.5°∠60°) for reactivation.

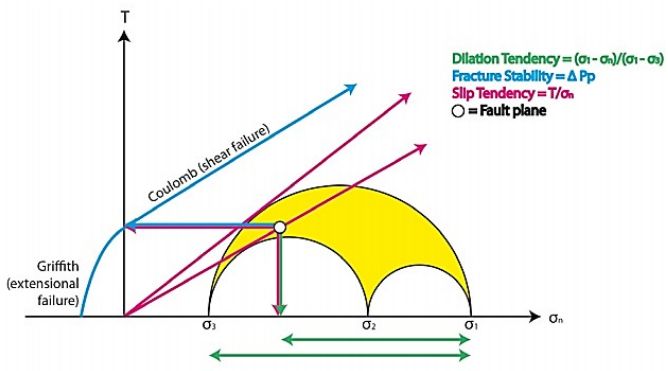

Fig. 12. Mohr circle Diagram

The faults E-W and NE-SW have slip tendency values that ranges from 0.3 to 0.4 suggesting that the tendency of the slip along this fault is less in the prevailing stress regime (Fig. 13). The dilation tendency value for the faults ranges from 0.5to0.6 (Fig. 15) and it shows that faults are more critically oriented for a greater tendency of dilation than slip. Both analyses show thatthe faults atreservoir depth are stable and reactivation chances are remote. The fracture stability attribute was calculated from knowledge of the in-situ stress field, fault rock failure envelope, pore pressure, and fault orientation. This method estimates the risk of fault reactivation, taking into account variations in fault cohesion and friction (Mildren et al, 2002, 2005). Results show that the lowest pore pressure increase

required to cause the cohensionless pre-existing faults to reactivate varies from 15 MPa in the normal regime case. As result of an increase in pore pressure before reaching failure is becoming greater at greater depth, the faults mapped at greater depth appear more stable than faults in the shallow level, and this is expected due to increasing confining stress with depth, which makes shear reactivation more difficult.

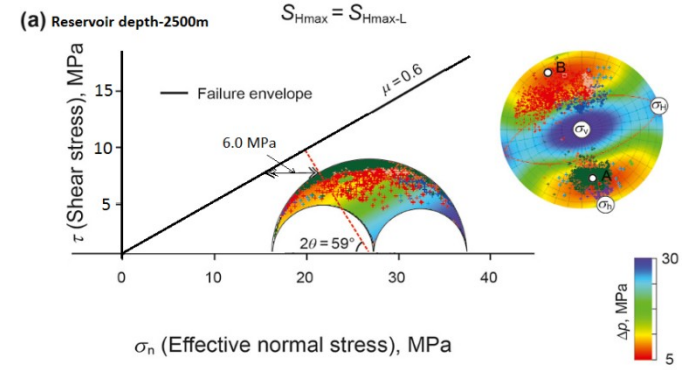

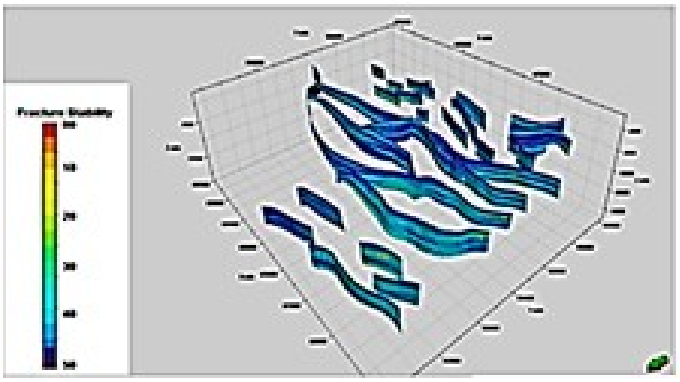

Fig. 13. (a) Mohr diagram and stereogram at 2500 m under the condition SHmax = SHmax-L; (b) Fracture stability distribution (cohesive strength of 1 MPa and an internal coefficient of friction of 0.3)

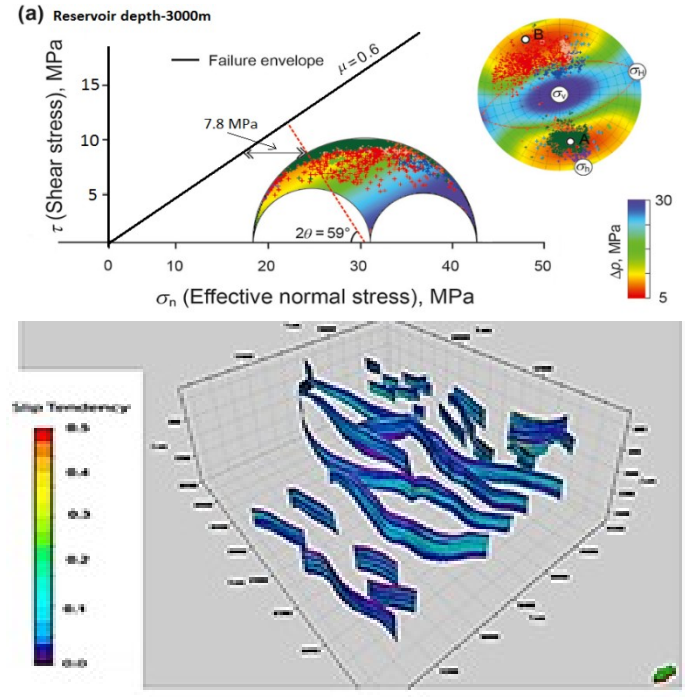

Fig. 14. (a) Mohr diagram and stereogram at 3000 m under the condition SHmax = SHmax-L; (b) Slip tendency distribution. Areas of high slip tendency are present on the trap-bounding faults 1 (black arrows). Maximum slip tendency is red and minimum slip tendency is blue.

Fault orientation and in-situ stress variation, however, play a major role locally, and can explain large variations in reactivation potential. From the structural framework established,the high-angle faults with southeast to northwest strike have the highest likelihood to reactivate under all normal stress regimes, whereas the north to south trending faults present the lowest risk. The evaluation results of the fracture stability model are shown in Figure 13.As depthincreases, there is no tangent between Mohr's circle and the failure envelope, and the fault stability inferred to be controlled by fault orientation, with faults that have a strike near ENE and a dip angle close to 60° being relatively unstable (Fig. 13). The Δp is 6.0MPa at 2500 m and 7.8MPa at 3000 m under the two boundary conditions of SHmax (Fig. 13) for optimally oriented faults. The results show that the Δp of optimally oriented faults increases with depth but is not affected by the change in SHmax (Φ).

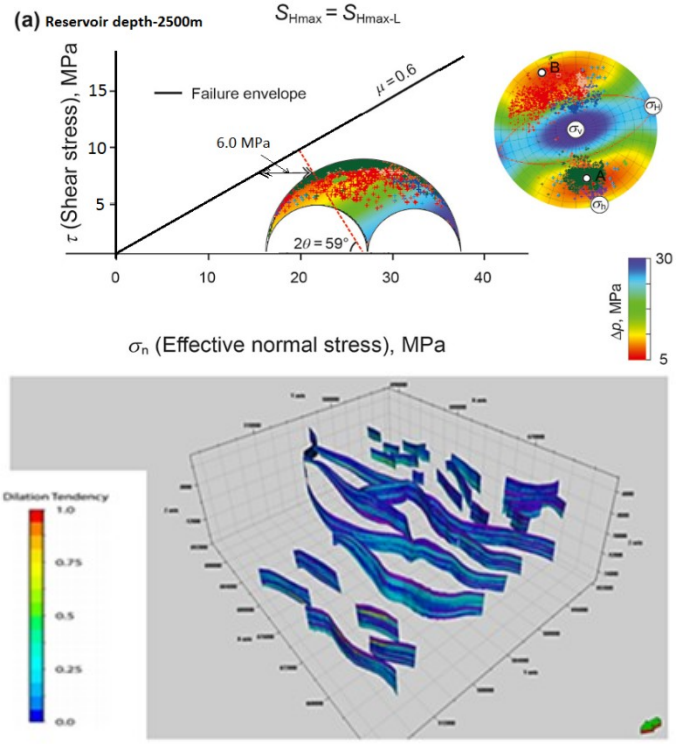

Fig. 13. (a) Mohr diagram and stereogram at 2500 m under the condition SHmax = SHmax-L; (b) Dilation tendency distribution. Maximum dilation tendency is red and minimum dilation tendency is blue

CONCLUSIONS

- The in situ stress regime in the field is between Sv>SHmax>Shmin and Sv ≈ SHmax>Shmin with SHmax oriented NEE–SWW to SEE–NWW. Based on the interpretation results of in-situ stress, both methods were employed to investigate the stability of faults. The traditional evaluation result of fault stability shows that all faults are stable.
- The vertical stress (Sv), derived by integrating bulk density logdata is equivalent to ~ 70- 75MPa/km at the top of the Agbada formation. SV is larger than 85 MPa/kmfor depths deeper than 2000m TVD.
- The magnitude of the least principal stress (S_{hmin}) is determined through LOT values conducted at various intervals of the selected offset wells. The minimum horizontal stress gradient at the top of the reservoir formation is equal to ~ 35- 40 MPa/km.
- Image logs have been analysed in order to identify the stress induced wellbore failures, useful for the determination of the S_{Hmax} azimuth. The S_{Hmax}azimuth has been interpreted to be ~ S95ºN.

- The magnitude of the maximum horizontal stress (S_{Hmax}) was constrained by performing stress modelling in intervals where wellbore failure were observed. This permitted confirmation of a normal faulting stress regime in the field and at the top of the Agbada Formation, the maximum horizontal stress magnitude is ~ 66.0 - 68.5 MPa/km.

Acknowledgments: The authors acknowledge the Nigerian Department of Petroleum Resources in is appreciated for providing data used in this study. Schlumberger is thanked for the software used in this study. The authors also thank Mr Magnus of SPDC and other anonymous reviewers for their comments and suggestions that improved the original manuscript.

Statements and declarations: We declare that we have no known competing financial interests or personal relationships that could have appeared to influence the work reported in this paper.

REFERENCES

Allen, J. R. L., 1965, Late Quaternary Niger Delta, and adjacent areas-sedimentary environments and lithofacies: AAPG Bulletin, v. 49, p. 547-600.

Adewole E. O. and D. Healy (2013), Quantifying in Situ Horizontal Stress in the Niger Delta Basin, Nigeria, GSTF Journal of Engineering Technology (JET), Vol. 2 No. 3. pp. 1-9.

Ahmadi, M.A.; Zendehboudi, S.; Lohi, A.; Elkamel, A.; Chatzis, I.(2013), Reservoir permeability prediction by neuralnetworks combined with hybrid genetic algorithm and particle swarm optimization. J. Geophys. Prospect, v. 61, pp. 582–598.

Akbar Ali A.H., Brown T., Delgado R., Lee D., Plumb D., Smirnov N., Marsden R., Prado-Velarde E., Ramsey L., Spooner D., Stone T. & Stouffer T., 2008. Watching Rocks Change – Mechanical Earth Modeling. Oilfield Review, 15, 2, 22–39.

Avbovbo, A.A., 1978, Tertiary lithostratigraphy ofNiger Delta: AAPG Bulletin, v. 62, p. 295-306.

Basir, H.M.; Javaherian, A.; Yaraki, M.T. (2013), Multi-attribute ant-tracking and neural network for fault detection: A case study of an Iranian oilfield. J. Geophys. Eng., v.10, pp. 1–10.

Bjørlykke K., Høeg K. &HaqueMondol M., 2010. Introduction to Geomechanics: Stress and Strain in Sedimentary Basins. [in:] Bjørlykke K. (ed.), Petroleum Geoscience: From sedimentary Environments to Rock Physics, Springer, Heidelberg, 281–298.

Bourne, S.J., Rijkels, L., Stephenson, B.J., Weber, A., Willemse, E.J.M., (2000), Predictive modellingof naturally fractured reservoirs using geomechanics and flow simulation. GeoArabiaV. 6, pp. 87-102.

Breyer, J. A.: The Eagle Ford Shale: a Renaissance in U.S. Oil Production: American Association of Petroleum Geologists, Memoir, 110, 399 pp., 2016.

Chopra, S., Marfurt, K.J., (2007), Seismic Attributes for Prospect Identification and Reservoir Characterization. Society of Exploration Geophysicists Publication, pp. 481.

Doust, H., and E. Omatsola, (1990),Niger Delta, in J.D. Edwards and P.A. Santagrossi, Eds., Divergent/passive margin basins: AAPG Memoir 45, pp. 201-238.

Fredrich, J.T., Arguello, J.G., Deitrick, G.L., de Rouffignac, E.P., (2000),Geomechanicalmodeling ofreservoir compaction, surface subsidence, and casing damage at the Belridge diatomite field. SPEReservoir Evaluation & Engineering 3, 348-359.

Fredrich, J.T., Coblentz, D., Fossum, A.F., Thorne, B.J., (2003), Stress Perturbations Adjacent to SaltBodies in the Deepwater Gulf of Mexico, SPE Annual Technical Conference and Exhibition. Societyof Petroleum Engineers, Denver, USA, pp. 5121-5134.

Ejedawe, J.E. (1981),, Patterns of incidence of oil reserves in Niger Delta basin: AAPG Bulletin, v. 65, pp. 1574-1585.

Ejedawe, J.E., Coker, S.J.L., Lambert-Aikhionbare, D.O., Alofe, K.B., and Adoh, F.O., (1984),Evolution of oil-generative window and oil and gas occurrence in Tertiary Niger Delta Basin: AAPG, v. 68, pp. 1744-1751.

Ekweozor, C.M., and E.M. Daukoru, 1984, Petroleum source-bed evaluation of Tertiary Niger Delta-reply: AAPG Bulletin, v.68, p. 390-394.

Evamy, B.D., J. Haremboure, P. Kamerling, W.A. Knaap, F.A. Molloy, and P.H. Rowlands, (1978), Hydrocarbon habitat of Tertiary Niger Delta: AAPG Bulletin, v. 64, pp. 59-66.

Hesthammer J. and H.Fossen (1997),Seismic attribute analysis in structural interpretation of the Gullfaks Field, northern North Sea, Petroleum Geoscience, Volume 3, pp. 13 – 26.

Gardner, G.H.F.; Gardner L.W. & Gregory A.R. (1974), Formation velocity and density -- the diagnostic basics for stratigraphic traps.

Ferrill D. A, K.J. Smart, and A.P. Morris (2020), Resolved stress analysis, failure mode, and fault-controlled fluid conduits, Solid Earth, V. 11, pp. 899–908.

Fredrich, J.T., Arguello, J.G., Deitrick, G.L., de Rouffignac, E.P., (2000),Geomechanicalmodeling of reservoir compaction, surface subsidence, and casing damage at the Belridge diatomite field. SPE Reservoir Evaluation & Engineering v.3, pp. 348-359.

Fredrich, J.T., Fossum, A.F., (2002), Large-scale three-dimensional geomechanicalmodeling of reservoirs; examples from California and the deepwater Gulf of Mexico. Oil & Gas Science and Technology 57, 423-441.

Fjaer, E., Holt, R.M., Horsrud, P., Raaen, A.M., Risnes, R., (2008), Petroleum Related Rock Mechanics,2 ed. Elsevier, pp. 515.

Gray, D., Anderson, P., Logel, J., F., D., Schmidt, D., Schmid, R., 2012.Estimation of stress andgeomechanical properties using 3D seismic data. First Break 30, 59-68.

Herwanger J. &Koutsabeloulis N., (2011).Building Reservoir Geomechanical Model. [in:] Seismic Geomechanics: How to Build and Calibrate Geomechanical Models using 3D and 4D Seismic Data, EAGE Publications, Houten, pp. 17–37.

Henk, A., 2009. Perspectives of geomechanical reservoir models – why stress is important. Oil Gas European Magazine v. 35, pp. 20-24.

Henk, A., Nemcok, M., 2008.Stress and fracture prediction in inverted half-graben structures.Journal of Structural Geology, v 30, pp. 81-97.

Jafari, A.; Babadagli, T.(2012), Estimation of equivalent fracture network permeability using fractal and statistical network properties. J. Pet. Sci. Eng.,pp. 92–93, pp. 110–123.

Jafari, A.; Kadkhodaie-Ilkhchi, A.; Sharghi, Y.; Ghanavati, K. (2012), Fracture density estimation from petrophysical log data using the adaptive neuro-fuzzy inference system. J. Geophys. Eng., v.9, pp. 105–114.

King G.E., (2012), Hydraulic Fracturing 101: What every Representative, Environmentalist, Regulator, Reporter, Investor, University Researcher, Neighbor and Engineer Should Know About Estimating Frack Risk and Improving Frack Performance in Unconventional Gas and Oil

Langhiand Reymond, (2005), Seismic Attributes Mapping of Late Palaeozoic Glacial Deposits on the Australian Northwest Shelf, Exploration Geophysics. V. 36, no. 2, pp. 224-233

Longuemare et al. (2002),Geomechanics in Reservoir Simulation: Overview of Coupling Methods and Field Case Study, Oil & Gas Science and Technology - Revue de l IFP v. 57 no.5 pp. 471-483.

Liu, E., Martinez, A., (2012), Seismic Fracture Characterization. Concepts and Practical Applications.Education Tour Series. EAGE Publications BV, pp. 279.

Marfurt, K.J., Chopra, S., (2006), Seismic Attribute Mapping of Structure and Stratigraphy. 2006 Distinguished Instructor Short Course. Distinguished Instructor Series, No. 9, pp. 226

Mildren S. D. ans J. Kaidi, (2002), Calibrating predictions of fault seal reactivation in the Timor Sea, The APPEA Journal, v,42, no. 1, pp,187-202

Mildren S.D., R.R. Hillis, P.J. Lyon, (2005), FAST: a new technique for geomechanical assessment of the risk of reactivation-related breach of fault seals P. Boult, J. Kaldi (Eds.), (In) Evaluating Fault and Cap Rock Seals: AAPG Hedberg Series, vol. 2 (2005), pp. 73-85.

Morley C. K. and Seusutthiya, K., (2007), Fault superposition and linkage resulting from stress changes during rifting: Examples

from 3D seismic data, PhitsanulokBsin, Thailand, Journal of Structural Geology, V.29 no.4, pp. 646-663.

Morris, A. P., Ferrill, D. A., and Henderson, D. B.: Slip tendencyanalysis and fault reactivation, Geology, 24, 275–278, 1996.

Nelson, R.A., (2001). Geologic Analysis of Naturally Fractured Reservoirs, second ed. Gulf Professional Publishing, pp. 332.

Narr, W., Schechter, D.W., Thompson, L.B., (2006), Naturally Fractured Reservoir Characterization. Society of Petroleum Engineers, pp. 115.

Orife, J.M., and A. A. Avbovbo, (1981), Stratigraphic and unconformity traps in the Niger Delta (abs.): AAPG Bulletin, v. 65, p. 967. https://doi.org/10.1306/2F91A0F7-16CE-11D7-8645000102C1865D.

Orlic, B., Wassing, B.B.T., 2013. A study of stress change and fault slip in producing gas reservoirs overlain by elastic and viscoelastic caprocks, Special Issue: New and Exciting Advances, 3 ed. Springer, Vienna, Austria, pp. 421-435.

SathyamoorthyS., Olatunbosun O., Sabatini D., OrekyehU., E. Olaniyan (2009), Society of Petroleum Engineers, Nigeria Annual International Conference and Exhibition, 3-5 August, Abuja, Nigeria. DOI https://doi.org/10.2118/128348-MS

Slatt R.M., 2011. Important geological properties of unconventional resource shales. Central European Journal of Geosciences, v.34, pp. 435–448.

Suarez-Rivera, R., Handwerger, D., Rodriguez Herrera, A., Herring, S., Stevens, K., Vaaland, G.D., Borgos, H., Marino, S., Paddock, D., (2013), Development of a Heterogeneous Earth Model in Unconventional Reservoirs, for Early Assessment of Reservoir Potential, 47th US Rock Mechanics / Geomechanics Symposium, San Francisco, USA.

van Wees, J.D., Orlic, B., van Eijs, R., Zijl, W., Jongerius, P., Schreppers, G.J., Hendriks, M., Cornu,T., (2000), Integrated 3D geomechanical modelling for deep subsurface deformation: a case study oftectonic and human-induced deformation in the eastern Netherlands, in: Nieuwland, D.A. (Ed.), NewInsights into Structural Interpretation and Modelling. Geological Society, London, pp. 313-328.

Vernik, L., Zoback, M.D., Brudy, M., (1992), Methodology and application of the wellbore breakout analysis in estimating the maximum horizontal stress magnitude in the KTB pilot hole.Scientific Drilling v.3, pp. 161-169.

Vidal-Gilbert, S., Nauroy, J.-F., Brosse, E., (2009), 3D geomechanical modelling for CO2 geologic storage in the Dogger carbonates of the Paris Basin. International Journal of Greenhouse Gas Control v. 3, pp. 288-299.

Vidal-Gilbert, S., Tenthorey, E., Dewhurst, D., Ennis-King, J., Van Ruth, P., Hillis, R., (2010), Geomechanical analysis of the Naylor Field, Otway Basin, Australia: Implications for CO_2 injection and storage. International Journal of Greenhouse Gas Control v. 4, pp. 827-839.

Walter, H.F.; Dresser, A. (1980), Evaluation of fractured reservoir rocks using geophysical well logs. In Proceedings of the SPE Unconventional Gas Recovery Symposium, Pittsburgh, PA, USA, pp. 18–21.

Yale, D.P., (2003), Fault and stress magnitude controls on variations in the orientation of in situ stress, in: Ameen, M. (Ed.), Fracture and In-Situ Stress Characterization of Hydrocarbon Reservoirs. Geological Society, London, pp. 55-64.

Zendehboudi, S.; Ahmadi, M.A.; Bahadori, A.; Shafiei, A.; Babadaghli, T. (2012), A developed smart technique to predict minimum miscible pressure—EOR implications. Can. J. Chem. Eng., v. 91, pp. 1325–1337.

Zoback, M.D., 2007. Reservoir Geomechanics. Cambridge University Press, pp. 461.

****